Modelica Based Transient Modeling of a Flash Tank Vapor Injection System and Experimental Validation

Hongtao Qiao
htqiao@umd.edu

Xing Xu

Vikrant Aute

Reinhard Radermacher

Modelica Based Transient Modeling of a Flash Tank Vapor Injection System and Experimental Validation

Hongtao QIAO[1]*, Xing XU[2], Vikrant AUTE[3], Reinhard RADERMACHER[4]

Center for Environmental Energy Engineering
Department of Mechanical Engineering, University of Maryland
College Park, MD 20742 USA
[1,3]Tel: 301-405-8726, [2]Tel: 301-504-5003, [4]Tel: 301-405-5286, Fax: 301-405-2025
Email: [1]htqiao@umd.edu, [2]xuxing@umd.edu, [3]vikrant@umd.edu, [4]raderm@umd.edu,

*Corresponding Author

ABSTRACT

The flash tank vapor injection cycle is widely used and has been proven effective for improving system performance compared with the conventional systems. A good control design for this type of cycle to make the system work properly under various operation conditions is a challenge and one often has to resort to experimental studies, which are time-consuming and costly. In this paper, a transient mathematical model for a flash tank vapor injection heat pump system with an economized scroll compressor is presented. The compressor model is a map-based model. The heat exchangers are modeled using the finite volume method. The valves are modeled using empirical correlations. The resulting equations are solved using a commercially available differential algebraic equation solver. The simulation results are compared against experimental data and the comparison indicates that the model can predict system transient behavior during startup reasonably well. Using this validated model, the impact of the upper-stage EEV opening is investigated.

1. INTRODUCTION

Flash tank vapor injection (FTVI) system has been gaining popularity recently since it was first introduced to the market in late 1970s. Its applications have expanded considerably to satisfy different needs, such as heating, cooling and refrigeration. FTVI system is superior to the conventional systems owing to its higher energy efficiency and lower discharge temperature as well as the flexibility in adjusting the capacity by altering the vapor injection ratio.

So far, there have been many experimental studies carried out to compare the performance of FTVI system to that of the conventional ones under different operating conditions. All these studies demonstrate that system capacity and COP can improve remarkably when vapor injection is applied. Xu *et al*. (2011a) conducted a comprehensive literature review on vapor injection systems. In the review, the authors compared the flash tank cycle with the internal heat exchanger cycle in detail and pointed out that the system control should be carefully devised for the former in order for the flash tank to maintain a proper liquid level. As a follow-up study, the same authors (Xu *et al*., 2011b) analyzed several different control scenarios for a flash tank heat pump system and experimentally investigated the feasibility of using the injection superheat to control the injection ratio.

Although the experimental approach is the most straightforward and reliable one to tackle the difficulties in the control design of the FTVI system, clearly it is too expensive and time-consuming. Countless tests need to be conducted even just in order to find an adequate combination of PID parameters for controllers. Under this circumstance, a numerical dynamic model becomes necessary. The use of numerical models can facilitate understanding the phenomena related to the problems and reduce the financial cost of control design. To the authors' best knowledge, however, full understanding of models to simulate the dynamic behavior of FTVI system is still lacking and many efforts are still needed to make further progress.

This paper introduces a first-principles model to simulate the transient behavior of a flash tank heating pump system during startup. In the meanwhile, the transient response of the system to a step change in the opening of the upper-stage EEV will be analyzed. In the future, the model can be expanded to include other transients for shutdown, frosting and defrosting.

2. SYSTEM DESCRIPTION

The studied system and its P-h diagram are shown in Figure 1. In the system, an economized scroll compressor is used. The hot vapor discharged by the compressor flows through the condenser coil where cooler air removes the heat from the vapor until it condenses into a subcooled liquid when exiting the condenser. Then the liquid refrigerant goes through the upper-stage expansion valve where the pressure decreases drastically. This process results in a vapor-liquid mixture entering the flash tank where the vapor and liquid separates. The separated saturated vapor is routed to the economizer port of the compressor and mixed with the refrigerant after the first stage compression, while the saturated liquid goes through another throttling process before flowing through the evaporator coil where it evaporates. The resulting refrigerant vapor returns to the compressor inlet. The vapor is then compressed and discharged at a higher temperature, thus completing a thermodynamic cycle.

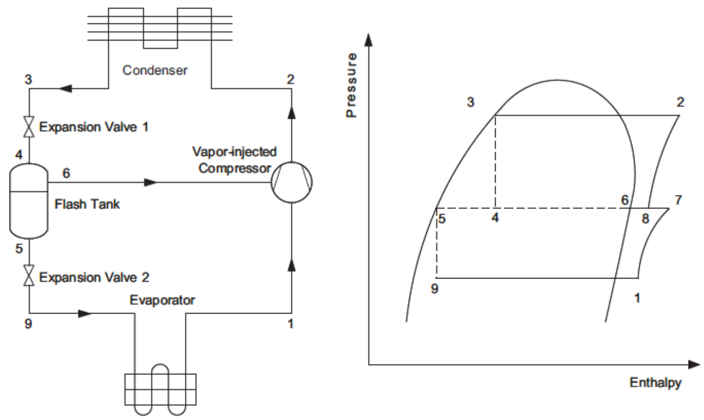

Figure 1: Schematic of a flash tank vapor injection system and P-h diagram (Wang, 2008)

3. MATHEMATICAL MODELS

3.1 Scroll Compressor

A scroll compressor with an economizer port is used in the studied system. Vapor injection can be turned on or turned off by opening or closing the solenoid valve before the economizer port on the injection line.

In the transient simulation, the compressor is generally treated as a quasi-steady state component because the timescales associated with the variation of the compressor mass flow rate are very small compared to timescales associated with heat exchanger and charge distribution. Therefore, a full-scaled physics-based compressor model that captures the detailed transients during the compression process is not necessary considering the computation cost (Winkler, 2009). As a result, a map-based compressor model is used in the study. The compressor is divided into two stages. The suction vapor is compressed in the first stage and then is mixed with the injected vapor from the economizer port. The mixture is further compressed in the second stage to the discharge pressure.

The polytropic compression process is well understood and its volumetric efficiency and compression power can be calculated using Equations (1) and (2), respectively

$$\eta_V = 1 - CL\left(R_p^{1/n} - 1\right) \tag{1}$$

$$W = Z_c N/60 \eta_V V_d p_s \left[R_p^{\frac{n-1}{n}} - 1\right] \tag{2}$$

In reality, the compression process is very complex and is influenced by many factors. Without loss of physical meaning, the format of the above equations is adopted but the coefficients are curve-fitted based on the experimental data to account for the deviation of an actual compression from the polytropic compression.

The modified equation for the volumetric efficiency is given by

$$\eta_V = c_1\left[1 - c_2\left(R_p^{c_3} - 1\right)\right] \tag{3}$$

While the modified calculation for the compression power is

$$W = c_4 V_d N / 60 \eta_V p_s \left[R_p^{c_5} - 1\right] \tag{4}$$

The specific enthalpy of the refrigerant leaving each stage is determined by

$$h_d = h_s + \beta \frac{W}{\dot{m}} \tag{5}$$

where β is an empirical constant and c_1-c_5 are curve-fitted coefficients.

3.2 Expansion Valves

An electric expansion valve (EEV) is used in the upper-stage and a thermostatic expansion valve (TXV) is used in the lower-stage. The EEV attempts to control the intermediate pressure and thus the injection ratio, while the TXV tries to maintain the refrigerant entering the compressor at a certain superheat. In general, saturated refrigerant vapor passes through the vapor line of the flash tank. In such a condition, the EEV is not able to function properly. To resolve this issue, an electric heater is installed on the vapor line to ensure full vaporization of possible liquid carryover by the injection flow and to obtain a modest injection superheat. This injection superheat signal can be sent back to the PID controller of the EEV to control the EEV opening.

Same as the compressor model, the dynamics of the valve itself are neglected. The mass flow rate through the valve is determined by the flow coefficient, the flow area, the inlet density and the pressure drop across the valve

$$\dot{m} = C_v A \sqrt{\rho_{in} \Delta p} \tag{6}$$

The area in the above equation is a function of the EEV opening that is adjusted by the PID controller until the injection superheat reaches to its setting point. Since the pressure and temperature of the injection flow are both measured on the vapor line, the superheat can be sensed instantaneously. Therefore, there is no need to add a delay for the superheat signal to the PID controller.

For the TXV, the superheat is sensed by the bulb attached on the suction line. Hence, there is an inevitable delay between the sensed superheat and the actual superheat due to the thermal inertia of the bulb and the heat transfer resistance between the substance in the bulb and the refrigerant flowing in the suction line.

The bulb is modeled as a lumped section and its temperature variation is given by

$$\frac{dT_b}{dt} + \frac{1}{\tau_b} T_b = \frac{1}{\tau_b} T_r \tag{7}$$

where $\tau_b = M_b C_b / UA$ is the time constant of the bulb temperature response.

The spring deflection needs to be known in order to find the effective flow area. The force exerted by the spring can be found from a force balance on the diaphragm. Here, we assume that the spring force is a linear function of the spring deflection, yielding

$$P_b - P_s = Ky + P_{offset} \tag{8}$$

where K is a constant determined by the diaphragm area and spring constant. P_{offset} is the initial spring force. Once the spring deflection is known, the effective flow area can be calculated based on the internal geometry of the valve. More details can be found in (Li *et al*., 2004).

3.3 Heat Exchangers

Transient heat exchanger models generally fall into one of two categories; namely phase-independent finite volume models and phase-dependent moving boundary models (Bendapudi *et al.*, 2008). In finite volume models, the heat exchanger is subdivided into a fixed number of constant volumes and the manner in which the heat exchanger is subdivided is independent of the refrigerant phase. In moving boundary models, the heat exchanger is subdivided based on the location of the phase transition points. The length of each region changes with time as the transition points move throughout the heat exchanger. Compared with finite volume models, moving boundary models are more efficient in terms of computation because they utilize fewer control volumes. However, when it comes to simulation of fast transient behavior, such as startup and shut-down operations, moving boundary models tend to have difficulty in making a continuous, smooth and stable transition in the solving process when flow phase forms or disappears.

In general, the heat exchanger is analyzed by dividing it into three sections, i.e. refrigerant flow, finned wall and the air stream. The conservation laws are applied to each of these three sections. In the present study, the finite volume approach is adopted and each tube and its associated fins are considered as a control volume, as shown in Figure 2. The models are mainly based on the following assumptions:

1) The air side is modeled as an incompressible fluid and thus the dynamics is negligible.
2) The refrigerant flow is one dimensional flow.
3) The refrigerant properties are considered uniform on the transverse section of the heat exchangers.
4) The axial heat conduction in the refrigerant flow direction is ignored.
5) In the two phase region, the liquid and the vapor are in thermodynamic equilibrium.
6) The potential energy and kinetic energy of the refrigerant are not taken into account.
7) The tubes and fins are modeled as a lumped section and thus the metal temperature is uniform in each control volume.

Based on the above assumptions, the governing equations for each control volume can be established.

<u>Refrigerant side</u>

$$V\left[\left(\frac{\partial\rho_r}{\partial p_r}\right)_h\frac{dp_r}{dt}+\left(\frac{\partial\rho_r}{\partial h_r}\right)_p\frac{dh_r}{dt}\right]=\dot{m}_{r,i}-\dot{m}_{r,o} \tag{9}$$

$$V\left[h_r\left(\frac{\partial\rho_r}{\partial p_r}\right)_h-1\right]\frac{dp_r}{dt}+V\left[h_r\left(\frac{\partial\rho_r}{\partial h_r}\right)_p+\rho_r\right]\frac{dh_r}{dt}=\dot{m}_{r,i}h_i-\dot{m}_{r,o}h_o-Q_{rw} \tag{10}$$

$$p_{r,i}-p_{r,o}+G_r^2\left(\frac{1}{\rho_{r,i}}-\frac{1}{\rho_{r,o}}\right)\mp\int_0^L f_z dz=0 \tag{11}$$

<u>Finned wall</u>

$$\left(MC_p\right)\frac{dT_w}{dt}=Q_{rw}-Q_{wa} \tag{12}$$

<u>Air side</u>

$$T_{a,o}=T_w-\left(T_w-T_{a,i}\right)exp\left(-\frac{\eta_f\alpha_o A_T}{\dot{m}_a c_{p,a}}\right) \tag{13}$$

$$X_{a,o}=X_{sat,w}-\left(X_{sat,w}-X_{a,i}\right)exp\left(-\frac{\eta_f\alpha_o A_T}{\dot{m}_a c_{p,a}Le^{2/3}}\right) \tag{14}$$

A staggered grid scheme is used to solve the equations on the refrigerant side because it can give better convergence properties in cases of dealing with pressure gradient. Explicitly, mass and energy balance are calculated in control volumes, whereas the momentum balance is calculated between control volumes (Tummescheit, 2002).

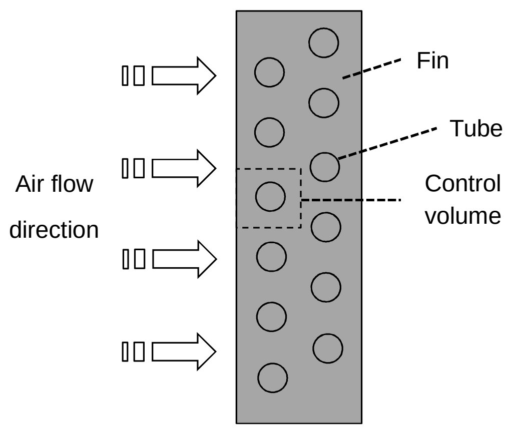

Figure 2: Control volume of the HX model

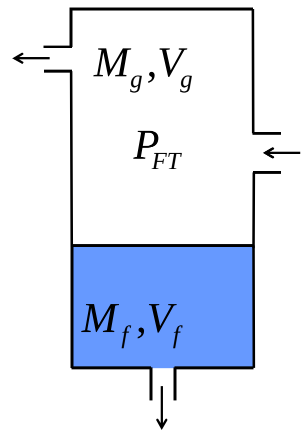

Figure 3: Schematic of a flash tank

3.4 Flash Tank

The liquid-vapor refrigerant mixture enters the flash tank and separates, shown in Figure 3. For the sake of simplicity, it is assumed in the present study that vapor and liquid perfectly separate although it is not the case in reality. Therefore, the flash tank is considered as a big control volume with one inlet and two outlets. Consequently, the governing equations can be written as follows

$$V\left[\left(\frac{\partial\rho_r}{\partial p_r}\right)_h \frac{dp_r}{dt} + \left(\frac{\partial\rho_r}{\partial h_r}\right)_p \frac{dh_r}{dt}\right] = \dot{m}_{r,i} - \dot{m}_{l,o} - \dot{m}_{v,o} \tag{15}$$

$$V\left[h_r\left(\frac{\partial\rho_r}{\partial p_r}\right)_h - 1\right]\frac{dp_r}{dt} + V\left[h_r\left(\frac{\partial\rho_r}{\partial h_r}\right)_p + \rho_r\right]\frac{dh_r}{dt} = \dot{m}_{r,i}h_i - \dot{m}_{l,o}h_{l,o} - \dot{m}_{v,o}h_{v,o} - Q_{rw} \tag{16}$$

The leaving enthalpies of the vapor and liquid streams are dependent upon the refrigerant state inside the flash tank. Here there are two cases that need to be taken into account, 1) there is liquid inside the flash tank; 2) there is no liquid inside the flash tank.

The criterion used to switch between these two cases is to compare the refrigerant mean density to the density of the saturated vapor at the same pressure. For the first case, the mean density is larger than that of the saturated vapor, then the vapor and liquid should perfectly separate.

$$h_{l,o} = h_l \tag{17}$$
$$h_{v,o} = h_v \tag{18}$$

For the second case, the mean density should be equal or smaller than that of the saturated vapor, and the leaving enthalpies of the streams should be both equal to the mean enthalpy.

$$h_{l,o} = h_{mean} \tag{19}$$
$$h_{v,o} = h_{mean} \tag{20}$$

3.5 Pipes

The governing equations for the pipe model are essentially the same as those for heat exchanger models except the air side heat transfer is in natural convection; readers are referred to the section for heat exchangers.

4. IMPLEMENTATION

In the present study, Modelica is chosen as the modeling language and the simulation environment is Dymola 7.4. In the recent years, Modelica/Dymola has been proven efficient for modeling complex thermo-fluid systems and a series of papers have been published in this area (Jesen and Tummescheit, 2002; Tummescheit, 2002; Casella and Schiavo, 2003; Elmqvist *et al*., 2003; Pfafferott and Schmitz, 2004). One of the most prominent advantages of using Modelica/Dymola is that users do not need to devote much effort on how to solve the mathematical DAEs generated by the models while can focus on the physical modeling. As a result, the modeling efficiency is significantly improved.

5. MODEL VALIDATION AND RESULTS

The component models were combined to construct a flash tank vapor injection system. R410A was selected as the working fluid. The components were sized based on the system studied by Xu *et al*. (2011b) and the detailed size information of each component can be found in the paper.

In the present study, only the heating mode was considered. Since the present study was not aimed to investigate the transients of frosting and defrosting, a frost-free operating condition was chosen, that is, the indoor temperature was 21°C (48% RH) and the outdoor temperature was 8.3°C (75% RH).

In this study, empirical correlations were used to predict the heat transfer coefficients and pressure drop on both refrigerant side and air side. All the correlations were summarized in Table 1 for completeness.

Table 1: Correlation Summary

	Air side	Refrigerant side	
Heat transfer coefficient	Kim *et al*. (1999)	Single phase	Gnielinski (1976)
		Condensing	Shah (1979)
		Evaporating	Jung-Radermacher (1989a)
Pressure drop	Kim *et al*. (1999)	Single phase	Blasius (Incropera & DeWitt 1996)
		Condensing	Lockhart-Martinelli (1949)
		Evaporating	Jung-Radermacher (1989b)

The system model was validated against the experimental data for two cases. The first case was a startup simulation case with a fixed EEV opening of 18%. The simulation lasted for 15 minutes after startup and all the outputs are shown in the following figures. Suction, discharge and intermediate pressure transients are shown in Figure 4. It can be observed that the system takes about 10 minutes to reach the steady-state. In the first 2 minutes, the discharge pressure increases rapidly, then gradually slows down the ascent and finally levels off. The intermediate pressure and the suction pressure have very similar transients. In the first 3 minutes, both pressures decline and thereafter rise up slowly. Compared to the discharge pressure, the transients of the intermediate and suction pressures are more benign than those of the discharge pressure because their steady-state values are closer to the initial system pressure. The steady-state values of the suction, intermediate and discharge pressures are 732kPa, 1220kPa and 2770kPa, respectively. The comparison between the simulation and the measured data shows that the model can predict the startup transients reasonably except that there are some disagreements in the first 2 minutes. This is understandable because the startup transients are very complex in the real life since they are affected greatly by the compressor in whose model lots of details are neglected in the present study. This necessitates a relatively detailed compressor model while still simple enough in order to account for the influence of internal heat transfer and the oil on the startup transients.

Figure 5 shows the change in the suction and discharge temperature as well as the suction superheat. It can be noted that the discharge temperature rises quickly in the first 4 minutes and then flattens out until it reaches to 361K after 10 minutes. Different from the discharge temperature, the suction temperature is quite stable during startup. It drops a little bit at the very beginning and then quickly recovers. There is no superheat at the first 30 seconds because there is not enough time for the liquid to vaporize in the evaporator coil till this point. The superheat increases quickly up to a peak value of 14K at 150 second. After that, it gradually drops down and maintains its steady-state value. The discrepancy in the steady-state superheat between the prediction and the measured data is about 0.7K. This is not that bad because the discrepancy directly comes from the under-prediction of the suction temperature shown in the same figure and the prediction for the suction pressure is still accurate.

Figure 6 illustrates the simulated changes in the heat load of two heat exchangers, compressor power and the liquid level in the flash tank. It can be seen that heat load and compressor power rise rapidly in the first 3 minutes and then gradually approach to the steady-state values after 10 minutes. The liquid in the flash tank quickly drains out after startup and maintains a very low level thereafter. Low liquid level was confirmed in the testing. As a matter of fact, bubbles were observed through the sight glass on the liquid line of the flash tank during the steady operation. This indicates that the liquid level is not high enough to separate the vapor from the liquid-vapor mixture and there is room to optimize the intermediate pressure thus improving the system performance.

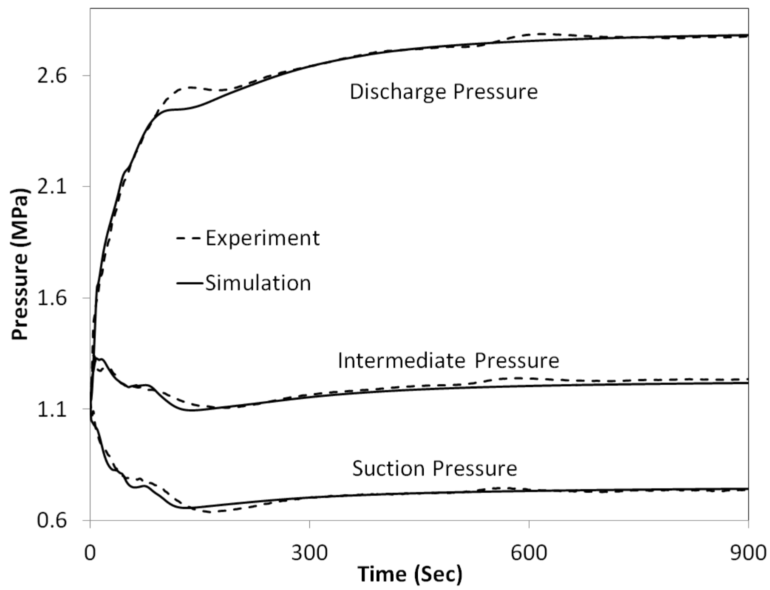

Figure 4: Suction, discharge and flash tank pressure change during startup

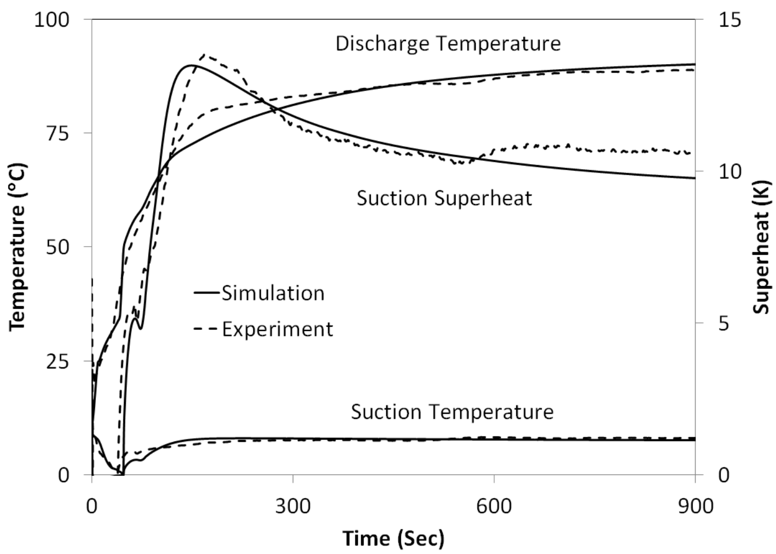

Figure 5: Suction and discharge temperature change and suction superheat change during startup

Figure 7 depicts the trend of the refrigerant redistribution in two heat exchangers and the flash tank during the startup since the refrigerant stored in these three components account for the majority of total charge. It can be noted that before startup, a great amount of liquid refrigerant sits in the evaporator coil; while very little refrigerant, mainly superheated vapor, is stored in the condenser coil. When the system starts up, the situation is reversed. Refrigerant is pumped into the condenser coil which holds up to 50% of total refrigerant, while the evaporator coil only holds less than 10%. Meanwhile, there is not much refrigerant left in the flash tank after startup, which is consistent with the change in the liquid level in the flash tank shown in the previous figure.

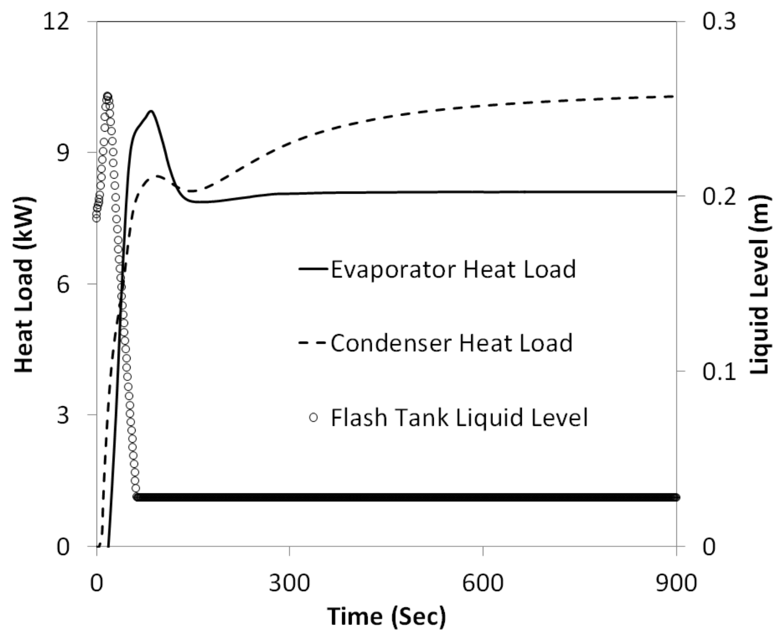

Figure 6: Heat load change and liquid level change in the flash tank

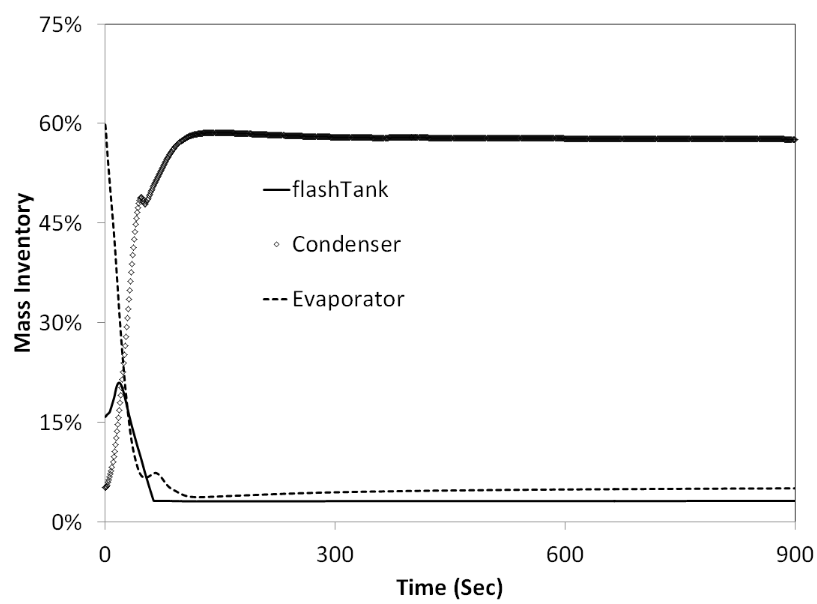

Figure 7: Mass inventory change during startup

The second case was to examine the transient response of the system to a step change in the opening of the upper-stage EEV. Starting from a steady-state condition, the EEV opening was changed from 18% to 20% and then to 25%. Figure 8 shows the responsive trends of pressures and the liquid level in the flash tank to the step change in EEV opening. It can be seen that when EEV opening increases, the discharge pressure decreases and the intermediate pressure increases. This is straightforward because an increase in EEV opening results in more mass flow rate through the valve and the pressure ratio must decline in order for the compressor to deliver an augmented refrigerant flow. Interestingly, the suction pressure nearly is stable when EEV opening is adjusted. This indicates that the EEV adjustment has very little effect on the suction pressure. A similar conclusion is also confirmed by

Zhang *et al*. (2009). In the meantime, EEV opening seems to have a significant impact on the liquid level in the flash tank. This can be explained by the fact that the variation in the discharge pressure will affect the length of the subcooled region in the condenser coil and the distribution of the active refrigerant inventory. When increasing EEV opening, the discharge pressure decreases and so is the refrigerant mass stored in the condenser coil. Then the surplus amount of inactive refrigerant mass will be stored in the flash tank. This phenomenon was also observed during the experiment.

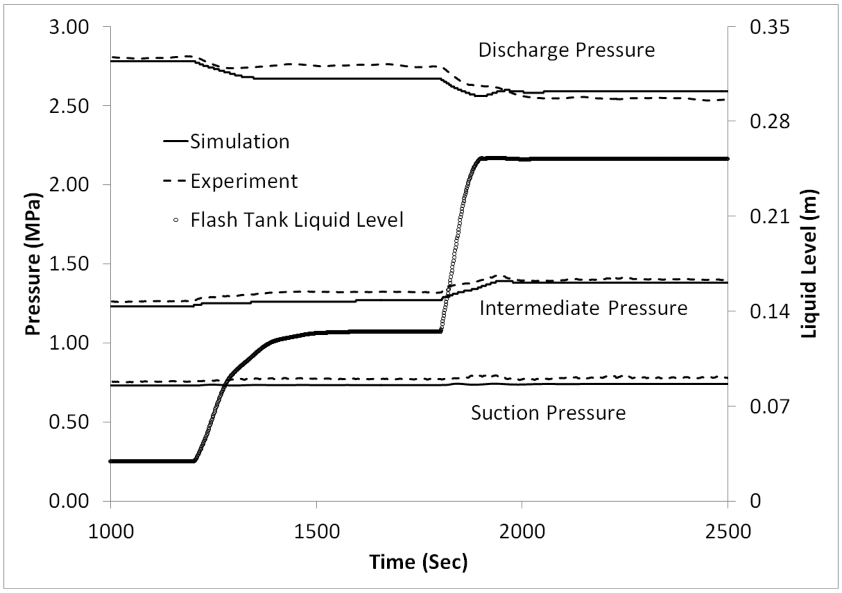

Figure 8: Transient response to a step change in EEV opening

6. CONCLUSIONS

A mathematical model has been developed for a flash tank vapor injection system with an economized scroll compressor. The comparison between the model prediction and the experimental data shows that the model can reasonably predict startup transients of the system. Using the validated model, the transient response of the system to a step change in the opening of the upper-stage EEV was studied. The result shows that the adjustment of the upper-stage EEV has little impact on the suction pressure. This is beneficial because it means that the system designers do not need to worry about the influence of the upper-stage EEV when they select the lower-stage TXV.

Even though the proposed model can provide a fairly good prediction, several possibilities exist for improving the model. A more detailed compressor model should be developed to capture the transients inside the compressor, including the heat transfer phenomena and oil effect. A more accurate void fraction calculation is needed because an accurate charge prediction is very difficult according to the authors' experience. Finally, the model could be modified to include the transients for shutdown, frosting and defrosting.

NOMENCLATURE

A	area	ρ	density
C_p	specific heat	$\dot{m}$	mass flow rate
CL	clearance volume ratio	η	efficiency
f	frictional loss coefficient	τ	time constant
G	mass flux	α	heat transfer coefficient
h	enthalpy	Δ	difference
K	gain		
L	length	Subscripts	

Le	Lewis number	a	air
M	mass	b	bulb
N	motor speed	d	discharge
p	pressure	f	liquid
Q	heat transfer rate	i	inlet
R_p	pressure ratio	mean	mean properties
T	temperature	o	outlet
t	time	r	refrigerant
V	volume	s	suction
W	power	sat	saturation
X	humidity ratio	v	vapor
y	distance	w	wall

REFERENCES

Bendapudi, S., Braun, J. E. and Groll, E. A., 2008. A Comparison of Moving-Boundary and Finite-Volume Formulation for Transients in Centrifugal Chillers. *Int. J. Refrig*. 31, 1437-1452.

Casella, F. and Schiavo, F., 2003. Modelling and simulation of heat exchangers in Modelica with finite element methods, *3rd International Modelica Conference*, Linkoping, Sweden.

Elmqvist, H., Tummescheit, H., Otter, M., 2003. Object-Oriented modeling of thermo-fluid systems, *3rd International Modelica Conference*, Linkoping, Sweden, 269-286.

Gnielinski, V., 1976. New equations for heat and mass transfer in turbulent pipe and channel flow. *Int. Chem. Eng*. 16 (2), 359-368.

Incropera, F.P. and DeWitt, D.P., *Introduction to Heat Transfer* (*3rd Ed*.). 1996. John Wiley & Sons, New York.

Jesen, J.M. and Tummescheit, H., 2002. Moving boundary models for dynamic simulations of two-phase flows, *2nd International Modelica Conference*, Oberpfaffenhofen, Germany; p.235-244.

Jung, D.S. and Radermacher, R., 1989a. A study of flow boiling heat transfer with refrigerant mixtures. *Int. J. Heat Mass Transfer* 32 (9), 1751-1764.

Jung, D.S. and Radermacher, R., 1989b. Prediction of pressure drop during horizontal annular flow boiling of pure and mixed refrigerants. *Int. J. Heat Mass Transfer* 32 (12), 2435-2446.

Kim, N.H., Youn, B., Webb, R.L., 1999. Air-Side Heat Transfer and Friction Correlations for Plain Fin-and-Tube Heat Exchangers with Staggered Tube Arrangements. *Trans. of ASME, J. Heat Transfer* 121, 662-667.

Li, H., Braun, J., Shen, B., 2004. Modeling adjustable throat-area expansion valves. *International Refrigeration and Air Conditioning Conference at Purdue*, West Lafayette, IN, USA, Paper No. 2130.

Lockhart, R.W. and Martinelli, R.C., 1949. Proposed Correlation of Data for Isothermal Two-Phase, Two-Component Flow in Pipes. *Chem. Eng. Progress* 45 (1), 39-48.

Pfafferott, T. and Schmitz, G., 2004. Modeling and transient simulation of CO2- refrigeration systems with Modelica. *Int. J. Refrig*. 27, 42-52.

Shah, M.M., 1979. A General Correlation for Heat Transfer during Film Condensation inside Pipes. *Int. J. Heat Mass Transfer* 22, 547-556.

Tummescheit, H., 2002. Design and Implementation of Object-Oriented Model Libraries using Modelica [PhD Dissertation]. Lund, Sweden: Department of Automatic Control Lund Institute of Technology.

Wang, X., 2008. Performance Investigation of Two-stage Heat Pump System with Vapor Injected Scroll Compressor. Ph.D. dissertation, University of Maryland College Park.

Winkler, J., 2009. Development of a component based simulation tool for the steady state and transient analysis of vapor compression systems. Ph.D. dissertation, University of Maryland College Park.

Xu, X., Hwang, Y., Radermacher, R., 2011a. Refrigerant injection for heat pumping/air conditioning systems: Literature review and challenges discussions. *Int. J. Refrig*. 34, 402-415.

Xu, X., Hwang, Y., Radermacher, R., 2011b. Transient and steady-state experimental investigation of flash tank vapor injection heat pump cycle control strategy. *Int. J. Refrig*. 34, 1922-1933.

Zhang, W.J., Zhang, C.L., Ding, G.L., 2009. Transient modeling of an air-cooled chiller with economized compressor. Part I: Model development and validation. *Applied Thermal Eng*. 29, 2396-2402.